

1 **Stable isotopic evidence for the excess leaching of unprocessed atmospheric**
2 **nitrate from forested catchments under high nitrogen saturation**

Weitian Ding¹, Urumu Tsunogai¹, Fumiko Nakagawa¹, Takashi Sambuichi¹, Masaaki
Chiwa², Tamao Kasahara³, Ken'ichi Shinozuka⁴

¹Graduate School of Environmental Studies, Nagoya University, Furo-cho, Chikusa-ku,
Nagoya 464-8601, Japan

²Kyushu University Forest, Kyushu University

³Faculty of Agriculture, Kyushu University

⁴River Basin Research Center, Gifu University, 1-1 Yanagido, Gifu, 501-1193, Japan

Corresponding author: Weitian Ding

Email: ding.weitian.v2@s.mail.nagoya-u.ac.jp

3 **Abstract**

4 Owing to the elevated loading of nitrogen through atmospheric deposition, some
5 forested ecosystems become nitrogen saturated, from which elevated levels of nitrate
6 are exported. The average concentration of stream nitrate eluted from upstream and
7 downstream of the Kasuya Research forested catchments (FK1 and FK2 catchments)
8 in Japan were more than 90 μM , implying that these forested catchments were under
9 nitrogen saturation. To verify that these forested catchments were under the nitrogen
10 saturation, we determined the export flux of unprocessed atmospheric nitrate relative to
11 the entire deposition flux ($M_{\text{atm}}/D_{\text{atm}}$ ratio) in these catchments, because the $M_{\text{atm}}/D_{\text{atm}}$
12 ratio has recently been proposed as a reliable index to evaluate nitrogen saturation in
13 forested catchments. Specifically, we determined the temporal variation in the
14 concentrations and stable isotopic compositions, including $\Delta^{17}\text{O}$, of stream nitrate in
15 the FK catchments for more than 2 years. In addition, for comparison, the same
16 parameters were also monitored in the Shiiba Research forested catchment (MY
17 catchment) in Japan during the same period, where the average stream nitrate
18 concentration was low, less than 10 μM . While showing the average nitrate
19 concentrations of 109.5, 90.9, and 7.1 μM in FK1, FK2, and MY, respectively, the
20 catchments showed average $\Delta^{17}\text{O}$ values of +2.6, +1.5, and +0.6 ‰ in FK1, FK2, and
21 MY, respectively. Thus, the average concentration of unprocessed atmospheric nitrate
22 ($[\text{NO}_3^-]_{\text{atm}}$) was estimated to be 10.8, 5.1, and 0.2 μM in FK1, FK2, and MY,
23 respectively, and the $M_{\text{atm}}/D_{\text{atm}}$ ratio was estimated to be 14.1, 6.6, and 1.3 % in FK1,

FK2, and MY, respectively. The estimated $M_{\text{atm}}/D_{\text{atm}}$ ratio in FK1 (14.1 %) was the highest ever reported from temperate forested catchments monitored for more than 1 year. Thus, we concluded that nitrogen saturation was responsible for the enrichment of stream nitrate in the FK catchments, together with the elevated NO_3^- leaching from the catchments. While the stream nitrate concentration ($[\text{NO}_3^-]$) can be affected by the amount of precipitation, the $M_{\text{atm}}/D_{\text{atm}}$ ratio is independent of the amount of precipitation; thus, the $M_{\text{atm}}/D_{\text{atm}}$ ratio can be used as a robust index for evaluating nitrogen saturation in forested catchments.

1 Introduction

Nitrate is important as a nitrogenous nutrient in the biosphere. Traditionally, forested ecosystems have been considered as nitrogen limited (Vitousek and Howarth, 1991). However, owing to the elevated loading of nitrogen through atmospheric deposition, some forested ecosystems become nitrogen saturated (Aber et al., 1989), from which elevated levels of nitrate are exported (Mitchell et al., 1997; Peterjohn et al., 1996). Such excessive leaching of nitrate from forested catchments degrades water quality and causes eutrophication in downstream areas (Galloway et al., 2003; Paerl and Huisman, 2009). Thus, evaluating the stage of nitrogen saturation in each forested catchment including its temporal variation, is critical for sustainable forest management, especially for forested ecosystems under high nitrogen deposition.

Both concentration and seasonal variation of stream nitrate have been used as indexes

to evaluate the nitrogen saturation of each forested catchment in past studies (Aber, 1992; Rose et al., 2015; Stoddard, 1994). A forested stream eluted from Fernow Experimental Forest USA, for instance, showed an elevated average nitrate concentration of 60 μM , along with the absence of a seasonal variation in the stream nitrate concentration, so the forest was classified into stage 3, the highest stage of nitrogen saturation (Rose et al., 2015).

However, using both the concentration level (high or low) and seasonal variation (clear or absent) of stream nitrate as indexes to evaluate nitrogen saturation has limitations, including the following (1) seasonal variation of soil nitrate can be buffered by groundwater with long residence time, so that the seasonal variation is unclear in stream nitrate concentration in Japan, even in normal forests under the nitrogen saturation stage of 0 (Mitchell et al., 1997); and (2) the stream nitrate concentration can be enriched or diluted depending on the volume of rainfall, so the concentration level can be high in low precipitation area irrespective of the stage of nitrogen saturation.

Nakagawa et al. (2018) lately proposed that the $M_{\text{atm}}/D_{\text{atm}}$ ratio, the export flux of unprocessed atmospheric nitrate (M_{atm}) relative to the deposition flux of NO_3^- (D_{atm}), can be an alternative, more robust index for evaluating nitrogen saturation in each forested catchment, because the $M_{\text{atm}}/D_{\text{atm}}$ ratio directly reflects the demand for atmospheric nitrate deposited onto each forested catchments as a whole, and thus reflect the nitrogen saturation in each forested catchment. That is, we can expect high $M_{\text{atm}}/D_{\text{atm}}$ ratios in forested catchments under nitrogen saturation and low $M_{\text{atm}}/D_{\text{atm}}$

ratios in forested catchments with nitrogen deficiency.

To estimate the $M_{\text{atm}}/D_{\text{atm}}$ ratio accurately and precisely in each forested catchment, the fraction of unprocessed atmospheric nitrate ($\text{NO}_3^-_{\text{atm}}$) in the stream needs to be estimated accurately and precisely. Triple oxygen isotopic compositions of nitrate ($\Delta^{17}\text{O}$) have recently been used as a conservative tracer of $\text{NO}_3^-_{\text{atm}}$ deposited onto each forested catchment (Inoue et al., 2021; Michalski et al., 2004; Nakagawa et al., 2018; Tsunogai et al., 2014; Ding et al., 2022), showing distinctively different $\Delta^{17}\text{O}$ from that of remineralized nitrate ($\text{NO}_3^-_{\text{re}}$), derived from organic nitrogen through general chemical reactions, including microbial N mineralization and microbial nitrification. While $\text{NO}_3^-_{\text{re}}$, the oxygen atoms of which are derived from either terrestrial O_2 or H_2O through microbial processing (i.e., nitrification), always shows the relation close to the “mass-dependent” relative relation between $^{17}\text{O}/^{16}\text{O}$ ratios and $^{18}\text{O}/^{16}\text{O}$ ratios; $\text{NO}_3^-_{\text{atm}}$ displays an anomalous enrichment in ^{17}O reflecting oxygen atom transfers from atmospheric ozone (O_3) during the conversion of NO_x to $\text{NO}_3^-_{\text{atm}}$ (Alexander et al., 2009; Michalski et al., 2003; Morin et al., 2011; Nelson et al., 2018). As a result, the $\Delta^{17}\text{O}$ signature defined by the following equation (Kaiser et al., 2007) enables us to distinguish $\text{NO}_3^-_{\text{atm}}$ ($\Delta^{17}\text{O} > 0$) from $\text{NO}_3^-_{\text{re}}$ ($\Delta^{17}\text{O} = 0$):

$$\Delta^{17}\text{O} = \frac{1 + \delta^{17}\text{O}}{(1 + \delta^{18}\text{O})^\beta} - 1 \quad (1)$$

where the constant β is 0.5279 (Kaiser et al., 2007), $\delta^{18}\text{O} = R_{\text{sample}}/R_{\text{standard}} - 1$ and R is the $^{18}\text{O}/^{16}\text{O}$ ratio (or the $^{17}\text{O}/^{16}\text{O}$ ratio in the case of $\delta^{17}\text{O}$ or the $^{15}\text{N}/^{14}\text{N}$ ratio in the case of $\delta^{15}\text{N}$) of the sample and each standard reference material. In addition, $\Delta^{17}\text{O}$ is almost

stable during “mass-dependent” isotope fractionation processes within terrestrial ecosystems. Therefore, while the $\delta^{15}\text{N}$ or $\delta^{18}\text{O}$ signature of $\text{NO}_3^-_{\text{atm}}$ can be overprinted by the biological processes subsequent to deposition, $\Delta^{17}\text{O}$ can be used as a robust tracer of unprocessed $\text{NO}_3^-_{\text{atm}}$ to reflect its accurate mole fraction within total NO_3^- , regardless of the progress of the partial metabolism (partial removal of nitrate through denitrification and assimilation) subsequent to deposition (Michalski et al., 2004; Nakagawa et al., 2013, 2018; Tsunogai et al., 2011, 2014, 2018).

Past studies reported that the maximum concentration of stream nitrate was 58.4 μM in the KJ forested catchment in Japan, with the maximum value of the $M_{\text{atm}}/D_{\text{atm}}$ ratio was 9.4 % (Nakagawa et al., 2018; Sase et al., 2022). Whether the index of the $M_{\text{atm}}/D_{\text{atm}}$ ratio can be applied to forested catchments, where the leaching of stream nitrate is much higher than the KJ forested catchment, remained unclarified. Besides, the advantages of the $M_{\text{atm}}/D_{\text{atm}}$ ratio within the past indexes of nitrogen saturation have not been discussed.

Chiwa (2021) has recently reported the enrichment of nitrate of more than 90 μM on the annual average in forested streams eluted from the FK catchments (FK1 and FK2) in Kasuya Research Forest, Kyushu University, Japan (Figs. 1a and 1b). The observed enrichment of stream nitrate implied that these forested catchments were under nitrogen saturation. Thus, in this study, we determined the $M_{\text{atm}}/D_{\text{atm}}$ ratio in the FK1 and FK2 forested catchments by monitoring both the concentration and $\Delta^{17}\text{O}$ of stream nitrate for more than 2 years to verify that these forested catchments were under nitrogen

saturation. For comparison, the MY forested catchment in Shiiba Research Forest, Kyushu University, Japan (Figs. 1a and 1c), was also monitored during the same period, where the average stream nitrate concentration was low (less than 10 μ M). Furthermore, the $M_{\text{atm}}/D_{\text{atm}}$ ratios in these forested catchments were compared with those reported in past studies to verify the reliability of the $M_{\text{atm}}/D_{\text{atm}}$ ratio as an index of nitrogen saturation.

2 Methods

2.1 Study sites

The FK forested catchments (33°38'N, 130°31'E) are located in a suburban area, about 15 km west of the Fukuoka metropolitan area (the fourth largest metropolitan area in Japan). The main plantation in these catchments was Japanese cedar/cypress (Table 1). The MY forested catchment (32°22'N, 131°09'E) is located in a rural area at the village of Shiiba in southern Japan's Central Kyushu Mountain range. This catchment is a mixed forest consisting of coniferous trees such as *Abies firma* Sieb. et Zucc., and *Tsuga sieboldii* Carr., and deciduous broadleaved trees such as *Quercus crispula* Blume, *Fagus crenata* Blume, and *Acer sieboldianum* Miq. Details on the studied forested catchments have been described in the past studies (Chiwa, 2020, 2021).

2.2 Sampling

The stream water eluted from the FK1 (14 ha), FK2 (62 ha), and MY (43 ha)

forested catchments were collected about once every month in principle from 2019/11 to 2021/12 (Fig. 1). At the FK catchments, stream water was collected at upstream (station A) and downstream (station B) locations (Fig. 1b). At the MY catchment, stream water was collected at station C (Fig. 1c). Samples of stream water to determine the concentration and stable isotopic compositions ($\delta^{15}\text{N}$, $\delta^{18}\text{O}$, and $\Delta^{17}\text{O}$) of stream nitrate were collected manually in bottles washed with deionized water before sampling and then rinsed at least twice with the sample before sampling at each sampling site.

2.3 Analysis

All the stream water samples were passed through a membrane filter (pore size 0.45 μm) within two days after sampling and stored in a refrigerator (4 $^{\circ}\text{C}$) until analysis. The concentrations of nitrate were measured by ion chromatography (Prominence HIC-SP, Shimadzu, Japan). To determine the stable isotopic compositions of nitrate in the stream water samples, nitrate in each sample was chemically converted to N_2O using a method originally developed to determine the $^{15}\text{N}/^{14}\text{N}$ and $^{18}\text{O}/^{16}\text{O}$ ratios of seawater and freshwater nitrate (McIlvin and Altabet, 2005) that was later modified (Konno et al., 2010; Tsunogai et al., 2011; Yamazaki et al., 2011). In brief, 11 mL of each sample solution was pipetted into a vial with a septum cap. Then, 0.5 g of spongy cadmium was added, followed by 150 μL of a 1 M NaHCO_3 solution. The sample was then shaken for 18-24 h at a rate of 2 cycles s^{-1} . Then, the sample solution (10 mL) was decanted into a different vial with a septum cap. After purging the solution using high-purity

helium, 0.4 mL of an azide–acetic acid buffer, which had also been purged using high-purity helium, was added. After 45 min, the solution was alkalized by adding 0.2 mL of 6 M NaOH. Then, the stable isotopic compositions ($\delta^{15}\text{N}$, $\delta^{18}\text{O}$, and $\Delta^{17}\text{O}$) of the N_2O in each vial were determined using the continuous-flow isotope ratio mass spectrometry (CF-IRMS) system at Nagoya University. The analytical procedures performed using the CF-IRMS system were the same as those detailed in previous studies (Hirota et al., 2010; Komatsu et al., 2008a). The obtained values of $\delta^{15}\text{N}$, $\delta^{18}\text{O}$, and $\Delta^{17}\text{O}$ for the N_2O derived from the nitrate in each sample were compared with those derived from our local laboratory nitrate standards to calibrate the values of the sample nitrate to an international scale and to correct for both isotope fractionation during the chemical conversion to N_2O and the progress of oxygen isotope exchange between the nitrate derived reaction intermediate and water (ca. 20 %). In this study, we adopted the internal standard method to calibrate the stable isotopic compositions of sample nitrate. Specifically, three kinds of the local laboratory nitrate standards were used in this study, which were named to be GG01 ($\delta^{15}\text{N} = -3.07$ ‰, $\delta^{18}\text{O} = +1.10$ ‰, and $\Delta^{17}\text{O} = 0$ ‰), HDLW02 ($\delta^{15}\text{N} = +8.94$ ‰, $\delta^{18}\text{O} = +24.07$ ‰), and NF ($\Delta^{17}\text{O} = +19.16$ ‰), which the GG01 and the HDLW02 were used to determine the $\delta^{15}\text{N}$ and $\delta^{18}\text{O}$ of stream nitrate, and the GG01 and the NF was used to determine the $\Delta^{17}\text{O}$ of stream nitrate. The GG01, HDLW02, and NF had been calibrated using the internationally distributed isotope reference materials (USGS 34 and USGS 35). The oxygen exchange rate between nitrate and water during the chemical conversion was calculated through Eq. (2):

$$\text{Oxygen exchange rate (\%)} = \Delta^{17}\text{O}(\text{N}_2\text{O})_{\text{NF}} / \Delta^{17}\text{O}(\text{NO}_3^-)_{\text{NF}} \quad (2)$$

where the $\Delta^{17}\text{O}(\text{N}_2\text{O})_{\text{NF}}$ denote the $\Delta^{17}\text{O}$ value of N_2O that convert from the NF nitrate, the $\Delta^{17}\text{O}(\text{NO}_3^-)_{\text{NF}}$ denote the $\Delta^{17}\text{O}$ value of NF nitrate ($\Delta^{17}\text{O} = +19.16 \text{ ‰}$) (Tsunogai et al., 2016; Nakagawa et al., 2013, 2018; Ding et al., 2022).

The $\delta^2\text{H}$ and $\delta^{18}\text{O}$ values of H_2O of the stream water samples were analyzed using the cavity ring-down spectroscopy method by employing an L2120-i instrument (Picarro Inc., Santa Clara, CA, USA) equipped with an A0211 vaporizer and autosampler. The errors (standard errors of the mean) in this method were $\pm 0.5 \text{ ‰}$ for $\delta^2\text{H}$ and $\pm 0.1 \text{ ‰}$ for $\delta^{18}\text{O}$. Both the VSMOW and standard light Antarctic precipitation (SLAP) were used to calibrate the values to the international scale. The $\delta^{18}\text{O}$ values of H_2O were used to calibrate the differences in $\delta^{18}\text{O}$ of H_2O between the samples and those our local laboratory nitrate standard samples (Tsunogai et al., 2010, 2011, 2014).

To determine whether the conversion rate from nitrate to N_2O was sufficient, the concentration of nitrate in the samples was determined each time we analyzed the isotopic composition using CF-IRMS based on the N_2O^+ or O_2^+ outputs. We adopted the $\delta^{15}\text{N}$, $\delta^{18}\text{O}$, and $\Delta^{17}\text{O}$ values only when the concentration measured via CF-IRMS correlated with the concentration measured via ion chromatography prior to isotope analysis within a difference of 10 %. We repeated the analysis of $\delta^{15}\text{N}$, $\delta^{18}\text{O}$, and $\Delta^{17}\text{O}$ values for each sample at least three times to attain high precision. All samples had a nitrate concentration of greater than $3.5 \text{ }\mu\text{M}$, which corresponded to a nitrate quantity greater than 35 nmol in a 10 mL sample. Thus, all isotope values presented in this study

have an error (standard error of the mean) better than ± 0.2 ‰ for $\delta^{15}\text{N}$, ± 0.3 ‰ for $\delta^{18}\text{O}$, and ± 0.1 ‰ for $\Delta^{17}\text{O}$.

Nitrite (NO_2^-) in the samples interferes with the final N_2O produced from nitrate because the chemical method also converts NO_2^- to N_2O (McIlvin and Altabet, 2005). Therefore, it is sometimes necessary to remove NO_2^- prior to converting nitrate to N_2O . In this study, however, we skipped the processes for removing NO_2^- because all the stream samples analyzed for stable isotopic composition had NO_2^- concentrations lower than the detection limit ($0.05 \mu\text{M}$).

2.4 Deposition rate of atmospheric nitrate

The annual deposition rate of atmospheric nitrate (D_{atm} ; total dry and wet deposition rate of atmospheric nitrate) in each catchment was estimated using the annual “bulk” deposition rate of atmospheric nitrate (D_{bulk}) calculated in Chiwa (2020) at each catchment by multiplying the volume-weighted mean concentration of nitrate in the bulk deposition samples collected every 2 weeks at each catchment for 10 years (from 2009/1 to 2018/12) by the annual amount of precipitation. The bulk deposition samples were those accumulated in a plastic bucket installed in an open site of each catchment 55 cm above the ground. The distances between the monitoring sites of bulk deposition in the FK1, FK2, and MY forested catchments and the stations of stream water sampling (stations A, B, and C) were 3.9, 2.9, and 4.5 km, respectively. The concentrations of nitrate in the bulk deposition samples were measured by ion chromatography.

The D_{bulk} determined through this method, however, is less than D_{atm} (Aikawa et al., 2003) because the dry deposition velocities of gases and particles on the water surface of the plastic bucket are smaller than those on the forest (Matsuda, 2008). Thus, we corrected the differences by using Eq. (3) to estimate D_{atm} from D_{bulk} :

$$D_{\text{atm}} = D_{\text{bulk}} - D_{\text{dry}}(\text{W}) + D_{\text{dry}}(\text{F}) \quad (3)$$

where $D_{\text{dry}}(\text{W})$ and $D_{\text{dry}}(\text{F})$ denote the annual dry deposition rates onto water and forest, respectively.

The $D_{\text{dry}}(\text{W})$ and $D_{\text{dry}}(\text{F})$ at each catchment were determined using an inferential method (Endo et al., 2011) through Eqs. (4) and (5), respectively:

$$D_{\text{dry}}(\text{W}) = [\text{NO}_3^-]_{\text{atm}}^{\text{gas}} \times V_{\text{gas}}(\text{W}) + [\text{NO}_3^-]_{\text{atm}}^{\text{p}} \times V_{\text{p}}(\text{W}) \quad (4)$$

$$D_{\text{dry}}(\text{F}) = [\text{NO}_3^-]_{\text{atm}}^{\text{gas}} \times V_{\text{gas}}(\text{F}) + [\text{NO}_3^-]_{\text{atm}}^{\text{p}} \times V_{\text{p}}(\text{F}) \quad (5)$$

where $[\text{NO}_3^-]_{\text{atm}}^{\text{gas}}$ denotes the concentration of gaseous nitrate in air; $[\text{NO}_3^-]_{\text{atm}}^{\text{p}}$ denotes the concentration of particle nitrate in air; $V_{\text{gas}}(\text{W})$ and $V_{\text{gas}}(\text{F})$ denote the deposition velocities of gaseous nitrate on the water surface and forest, respectively; and $V_{\text{p}}(\text{W})$ and $V_{\text{p}}(\text{F})$ denote the deposition velocities of particulate nitrate on the water surface and forest, respectively. Those determined by Chiwa (2010) using the annular denuder method from 2006/5 to 2007/4 were used for the $[\text{NO}_3^-]_{\text{atm}}^{\text{gas}}$ and $[\text{NO}_3^-]_{\text{atm}}^{\text{p}}$ in the FK catchments. Those determined by the National Institute for Environmental Studies (Environmental Laboratories Association of Japan, 2017) using the filter-pack method at Miyazaki (31°83'N, 131°42'E) from 2011 to 2017 were used for the $[\text{NO}_3^-]_{\text{atm}}^{\text{gas}}$ and $[\text{NO}_3^-]_{\text{atm}}^{\text{p}}$ in the MY catchment. The $V_{\text{gas}}(\text{F})$, $V_{\text{gas}}(\text{W})$, $V_{\text{p}}(\text{F})$, and $V_{\text{p}}(\text{W})$ of each

catchment were determined by applying the estimation file for dry deposition (Matsuda, 2008; http://www.hro.or.jp/list/environmental/research/ies/katsudo/acid_rain/kanseichinchaku/kanseichinchaku.html), where V_{gas} and V_p were calculated using the meteorological data of wind speed, temperature, humidity, radiation, and cloud amount and land use. The meteorological data monitored by Japan Meteorological Agency at the nearest Fukuoka station (33°34'N, 130°22'E) and Miyazaki station (31°56'N, 131°24'E) from 2009 to 2021 were used for the FK and MY catchments, respectively. The forested land use of 100 % was chosen for each area.

2.5 Flux of stream water

The flux of stream water (F_{stream}) in each catchment was not measured fully in this study. Instead, the water balance in each catchment was used to estimate F_{stream} , assuming that the outflux of water from the study catchments to deep groundwater was negligible:

$$F_{\text{stream}} = P - E \quad (6)$$

where P denotes the annual average precipitation and E denotes the annual evapotranspiration flux of water in each catchment. In this paper, the equation obtained by Komatsu et al. (2008) was used to estimate the E of the FK and MY catchments. Details on this equation are shown below.

Komatsu et al. (2008) compiled the annual flux of evapotranspiration determined in

43 forested catchments in Japan and found that E shows a positive correlation with the average temperature (T_{avg}) of each catchment. Thus, they proposed the modeled relation of $E \text{ (mm)} = 31.4T_{avg} \text{ (}^{\circ}\text{C)} + 376$ to estimate E in each forested catchment in Japan, where the standard error of 162.3 mm was included in the estimated evapotranspiration flux (E).

2.6 Concentration of unprocessed $\text{NO}_3^-_{\text{atm}}$ in each water sample

The $\Delta^{17}\text{O}$ data of nitrate in each sample was used to estimate the concentration of $\text{NO}_3^-_{\text{atm}}$ ($[\text{NO}_3^-_{\text{atm}}]$) in each water sample by applying Eq. (7):

$$[\text{NO}_3^-_{\text{atm}}]/[\text{NO}_3^-] = \Delta^{17}\text{O}/\Delta^{17}\text{O}_{\text{atm}} \quad (7)$$

where $[\text{NO}_3^-_{\text{atm}}]$ and $[\text{NO}_3^-]$ denote the concentrations of $\text{NO}_3^-_{\text{atm}}$ and nitrate (total) in each water sample, respectively, and $\Delta^{17}\text{O}_{\text{atm}}$ and $\Delta^{17}\text{O}$ denote the $\Delta^{17}\text{O}$ values of $\text{NO}_3^-_{\text{atm}}$ and nitrate (total) in the stream water sample, respectively. In this study, we used the annual average $\Delta^{17}\text{O}$ value of $\text{NO}_3^-_{\text{atm}}$ determined at the Sado-Seki monitoring station in Japan (Sado Island; Fig. 1a) from April 2009 to March 2012 ($\Delta^{17}\text{O}_{\text{atm}} = +26.3 \text{ ‰}$; Tsunogai et al., 2016) for $\Delta^{17}\text{O}_{\text{atm}}$ in Eq. (7) to estimate $[\text{NO}_3^-_{\text{atm}}]$ in the stream. We allow for an error range of 3 ‰ in $\Delta^{17}\text{O}_{\text{atm}}$, where the factor changes in $\Delta^{17}\text{O}_{\text{atm}}$ from +26.3 ‰ caused by both areal and seasonal variations in the $\Delta^{17}\text{O}$ values of $\text{NO}_3^-_{\text{atm}}$ have been considered (Nakagawa et al., 2018; Tsunogai et al., 2016; Ding et al., 2022).

The annual export flux of unprocessed $\text{NO}_3^-_{\text{atm}}$ per unit area of the catchment (M_{atm})

was determined by applying Eq. (8):

$$M_{\text{atm}} = [\text{NO}_3^-]_{\text{atm}} \times F_{\text{stream}} \quad (8)$$

where $[\text{NO}_3^-]_{\text{atm}}$ denotes the annual average $[\text{NO}_3^-]$ in each stream. The index of nitrogen saturation ($M_{\text{atm}}/D_{\text{atm}}$ ratio) was calculated by dividing M_{atm} with D_{atm} in each catchment.

2.7 Concentration and isotopic compositions of stream nitrate eluted only from the FK2 catchment

The concentration and isotopic compositions ($\delta^{15}\text{N}$, $\delta^{18}\text{O}$, and $\Delta^{17}\text{O}$) of stream nitrate determined at the station B were the mixture of those eluted from FK1 and FK2 catchments (Fig. 1b). Assuming that the stream nitrate eluted from FK1 catchment was stable during the flow path from station A to station B. The concentration of stream nitrate eluted from the FK2 catchment was determined by applying Eq. (9):

$$[\text{NO}_3^-]_{\text{FK2}} = ([\text{NO}_3^-]_{\text{FK1+FK2}} * F_{\text{FK1+FK2}} - [\text{NO}_3^-]_{\text{FK1}} * F_{\text{FK1}}) / F_{\text{FK2}} \quad (9)$$

where F_{FK1} , F_{FK2} , and $F_{\text{FK1+FK2}}$ denote the flux of stream water eluted from the FK1, FK2 (only), and FK1+FK2 catchment, respectively. $[\text{NO}_3^-]_{\text{FK1}}$, $[\text{NO}_3^-]_{\text{FK2}}$, and $[\text{NO}_3^-]_{\text{FK1+FK2}}$ denote the concentration of stream nitrate eluted from the FK1, FK2 (only), and FK1+FK2 catchment, respectively. In this study, the flow rates measured at stations A and B on 2021/01/15 by using the salt dilution method (Sappa et al., 2015) was used for F_{FK1} (0.85 L/s) and $F_{\text{FK1+FK2}}$ (4.75 L/s), respectively, and the measured $[\text{NO}_3^-]$ at stations A and B was used for $[\text{NO}_3^-]_{\text{FK1}}$ and $[\text{NO}_3^-]_{\text{FK1+FK2}}$, respectively.

Because the relation between the measured flow rates was comparable with the relation between the catchment area of FK1 (14 ha) and that of FK1+FK2 (76 ha), we concluded that the measured flow rates of 0.85 L/s and 4.75 L/s were reasonable as for those representing the F_{FK1} and $F_{FK1+FK2}$, respectively. According to the mass balance of water, we can estimate the F_{FK2} eluted from the FK2 catchment only to be 3.90 L/s.

Assuming that the stream nitrate eluted from FK1 catchment was stable during the flow path from station A to station B, the $\delta^{15}N$, $\delta^{18}O$, and $\Delta^{17}O$ values of stream nitrate eluted from the FK2 catchment only were determined by applying Eq. (10):

$$\delta_{FK2} = (\delta_{FK1+FK2} * [NO_3^-]_{FK1+FK2} * F_{FK1+FK2} - \delta_{FK1} * [NO_3^-]_{FK1} * F_{FK1}) / ([NO_3^-]_{FK2} * F_{FK2}) \quad (10)$$

where δ_{FK1} , δ_{FK2} , and $\delta_{FK1+FK2}$ denote the $\delta^{15}N$ (or $\delta^{18}O$ or $\Delta^{17}O$) of stream nitrate eluted from the FK1, FK2, and FK1+FK2 catchment, respectively. The $\delta^{15}N$ (or $\delta^{18}O$ or $\Delta^{17}O$) values of stream nitrate measured at stations A and B were used for δ_{FK1} and $\delta_{FK1+FK2}$, respectively.

3 Results

3.1 Deposition rate of atmospheric nitrate

The mean annual precipitation (P) from 2009 to 2021 was 1777 mm and 3981 mm for FK and MY catchments, respectively (Chiwa, 2020; Chiwa, personal communication, September 21, 2022). The mean annual temperature (T_{avg}) was reported to be 15.9 °C and 10.8 °C for FK and MY catchments, respectively (Chiwa,

2020). Based on these data, the annual flux of stream water (F_{stream}) was estimated to be 902.0 ± 162.3 mm at FK catchments and 3266.1 ± 162.3 mm at MY catchment, respectively, using Eq. (6).

Chiwa (2020) reported the annual bulk deposition rates of atmospheric nitrate (D_{bulk}) to be $34.0 \text{ mmol m}^{-2} \text{ year}^{-1}$ at FK catchments and $24.2 \text{ mmol m}^{-2} \text{ year}^{-1}$ at MY catchment. On the other hand, the annual dry deposition rate of atmospheric nitrate (D_{dry}) deposited on the forest ($D_{\text{dry}}(\text{F})$) and on the water surface ($D_{\text{dry}}(\text{W})$) were estimated to be $39.9 \text{ mmol m}^{-2} \text{ year}^{-1}$ and $4.1 \text{ mmol m}^{-2} \text{ year}^{-1}$, respectively, at FK catchments, and $18.4 \text{ mmol m}^{-2} \text{ year}^{-1}$ and $2.4 \text{ mmol m}^{-2} \text{ year}^{-1}$, respectively, at MY catchment. As a result, D_{atm} was estimated to be $69.3 \text{ mmol m}^{-2} \text{ year}^{-1}$ at FK catchments and $40.1 \text{ mmol m}^{-2} \text{ year}^{-1}$ at MY catchment, using Eq. (3).

3.2 Concentration and isotopic composition of stream nitrate

The concentrations of stream nitrate eluted from the FK1, FK2 (only), and MY catchments ranged from $97.5 \text{ }\mu\text{M}$ to $121.3 \text{ }\mu\text{M}$, from $65.7 \text{ }\mu\text{M}$ to $148.5 \text{ }\mu\text{M}$, and from $3.5 \text{ }\mu\text{M}$ to $15.3 \text{ }\mu\text{M}$, respectively, with the average concentrations of $109.5 \text{ }\mu\text{M}$, $90.9 \text{ }\mu\text{M}$, and $7.3 \text{ }\mu\text{M}$, respectively, and the standard deviations (SD) of $6.3 \text{ }\mu\text{M}$, $18.5 \text{ }\mu\text{M}$, and $3.0 \text{ }\mu\text{M}$, respectively, which corresponds to the coefficients of variation (CV) of 5.7% , 20.4% , and 40.7% , respectively (Fig. 2a). All catchments showed no clear seasonal variation during the observation periods. The variation ranges and the average concentrations of stream nitrate eluted from the three catchments agreed well with the

past observations performed in the same catchments (Chiwa, 2021).

The stable isotopic compositions of stream nitrate eluted from the FK1, FK2 (only), and MY catchments ranged from -0.9‰ to $+1.5\text{‰}$, from -1.4‰ to $+5.8\text{‰}$, and from -0.8‰ to $+2.4\text{‰}$, respectively, for $\delta^{15}\text{N}$ (Fig. 2b), from $+3.9\text{‰}$ to $+8.5\text{‰}$, from -2.2‰ to $+2.8\text{‰}$, and from -5.6‰ to $+1.7\text{‰}$, respectively, for $\delta^{18}\text{O}$ (Fig. 2c), and from $+2.0\text{‰}$ to $+3.3\text{‰}$, from $+0.6\text{‰}$ to $+2.2\text{‰}$, and from $+0.2\text{‰}$ to $+1.0\text{‰}$, respectively, for $\Delta^{17}\text{O}$ (Fig. 2d), with no clear seasonal variation during the observation periods. The concentration-weighted averages for the $\delta^{15}\text{N}$, $\delta^{18}\text{O}$, and $\Delta^{17}\text{O}$ values of stream nitrate were $+0.2\text{‰}$, $+6.4\text{‰}$, and $+2.6\text{‰}$, respectively, at FK1, $+1.0\text{‰}$, $+0.5\text{‰}$, and $+1.5\text{‰}$, respectively, at FK2, $+0.7\text{‰}$, -2.5‰ , and $+0.6\text{‰}$, respectively, at MY.

3.3 Concentration of unprocessed atmospheric nitrate and the $M_{\text{atm}}/D_{\text{atm}}$ ratio in each catchment

The concentration of unprocessed atmospheric nitrate ($[\text{NO}_3^-]_{\text{atm}}$) in the streams eluted from the FK1, FK2 (only), and MY catchments ranged from 8.64 to $14.30\text{ }\mu\text{M}$, from 2.27 to $10.71\text{ }\mu\text{M}$, and from 0.03 to $0.46\text{ }\mu\text{M}$ with the average concentration of 10.80 ± 1.65 , 5.06 ± 0.92 , and $0.16 \pm 0.05\text{ }\mu\text{M}$, respectively, even though these studied catchments showed little seasonal variations during the observation periods (Fig. 2e).

The annual export flux of nitrate (M_{total}), the annual export flux of NO_3^- (M_{atm}), and the $M_{\text{atm}}/D_{\text{atm}}$ ratio were $98.8 \pm 17.8\text{ mmol m}^{-2}\text{ year}^{-1}$, $9.7 \pm 2.3\text{ mmol m}^{-2}\text{ year}^{-1}$, and $14.1 \pm 4.4\text{ }\%$ at FK1 catchment, respectively, $82.0 \pm 14.8\text{ mmol m}^{-2}\text{ year}^{-1}$, 4.6 ± 1.2

mmol m⁻² year⁻¹, and 6.6 ± 2.1 % at FK2 catchment, respectively, 23.7 ± 1.2 mmol m⁻² year⁻¹, 0.5 ± 0.2 mmol m⁻² year⁻¹, and 1.3 ± 0.5 % at MY catchment, respectively (Table 2).

4 Discussion

4.1 Deposition rate of atmospheric nitrate at the study catchments

Based on the air monitoring data determined at the stations of Fukuoka (33°51'N, 130°50'E) and Miyazaki (31°83'N, 131°42'E) from 2011 to 2017, the Environmental Laboratories Association of Japan (2017) reported D_{atm} to be 57.8 mmol m⁻² year⁻¹ at Fukuoka and 49.1 mmol m⁻² year⁻¹ at Miyazaki. Those values are consistent with the D_{atm} estimated in this study (69.3 and 40.1 mmol m⁻² year⁻¹ at the FK and MY catchments, respectively), within a difference of approximately 20 %. Thus, we concluded that the D_{atm} estimated in this study was reliable within the error margin of 20 % (Table 2). Because the D_{atm} determined at the FK catchments was the highest among the forested catchments in Table 3, we further compared the D_{atm} of the FK catchments with those from the other air monitoring stations in Japan reported in past studies, along with that of the MY catchment (Table S1). While the D_{atm} of the MY catchment corresponded to the average level among the sites compiled in Table S1, the D_{atm} of the FK catchments exceeded the average level significantly. In addition, the D_{atm} of the FK catchments corresponded to one of the highest among the Japanese forested areas (Table S1). All the catchments in Japan can be suffered from the long-range

transport of air pollutants derived from megacities in East Asian region (Chiwa, 2021; Chiwa et al., 2012 and 2013). In addition, the shorter transport distance from the Fukuoka metropolitan area (total population: 1.62 million people; population density: 4715 people/km²) may be mainly responsible for the D_{atm} higher in FK than in MY, because the FK catchments are only 15 km west of the Fukuoka metropolitan area.

4.2 Excess leaching of unprocessed atmospheric nitrate from FK catchments

The isotopic compositions ($\delta^{15}\text{N}$, $\delta^{18}\text{O}$, and $\Delta^{17}\text{O}$) of stream nitrate eluted from the FK and MY catchments were typical for those eluted from forested catchments (Hattori et al., 2019; Huang et al., 2020; Nakagawa et al., 2013, 2018; Riha et al., 2014; Sabo et al., 2016; Tsunogai et al., 2014, 2016). The striking features found in the FK catchments were that, in addition to the high $[\text{NO}_3^-]$ and high M_{total} that had been clarified in a past study (Chiwa, 2021), both $[\text{NO}_3^-]_{\text{atm}}$ and M_{atm} in FK were higher than those eluted from MY (Table 2). Especially, the average $[\text{NO}_3^-]_{\text{atm}}$ in the stream eluted from the FK1 catchment was the highest ever reported in forested streams determined through continuous monitoring for more than 1 year (Bostic et al., 2021; Bourgeois et al., 2018b, 2018a; Hattori et al., 2019; Huang et al., 2020; Nakagawa et al., 2018; Rose et al., 2015; Sabo et al., 2016; Tsunogai et al., 2014, 2016).

The observed high $[\text{NO}_3^-]_{\text{atm}}$ in the stream eluted from the FK1 catchment could be caused just by the high $[\text{NO}_3^-]_{\text{atm}}$ in deposition in the catchment. Thus, we compiled all past data ever reported in forested streams through continuous monitoring in Table 3,

where the data of average $[\text{NO}_3^-]$, average $[\text{NO}_3^-]_{\text{atm}}$, M_{atm} , M_{total} , D_{atm} , and $M_{\text{atm}}/D_{\text{atm}}$ ratio were included for comparison. The result showed that the $M_{\text{atm}}/D_{\text{atm}}$ ratio, along with M_{atm} , was the highest as well in the FK1 catchment among the forested catchments (Table 3).

Elevated loading of nitrogen through atmospheric deposition was responsible for the occurrence of nitrogen saturation in forest ecosystems, from which elevated levels of nitrate are exported (Aber et al., 1989). Nakagawa et al. (2018) proposed that the $M_{\text{atm}}/D_{\text{atm}}$ ratio can be an index for evaluating the nitrogen saturation in each forested catchment, because the $M_{\text{atm}}/D_{\text{atm}}$ ratio directly reflects the present demand for atmospheric nitrate deposited in each forested catchment, and thus reflects the nitrogen saturation in each forested catchment. The high $M_{\text{atm}}/D_{\text{atm}}$ ratios observed in the FK catchments implied that the demand for atmospheric nitrate was low in the FK catchments and that the stages of nitrogen saturation at the FK catchments were higher than those at other forested catchments. That is, the nitrogen saturation at the FK catchments was responsible for the observed high $[\text{NO}_3^-]$ and high M_{total} at the FK catchments than at MY and any other catchment ever studied (Table 3).

The stand age of forests can affect the retention or loss of N (Fukushima et al., 2011; Ohnishi and Mitchell, 1997). Fukushima et al. (2011) evaluated N uptake rates of Japanese cedars at different ages (5-89 years old) and demonstrated that the N uptake rates of Japanese cedars were higher in younger stands ($53 \text{ kg N ha}^{-1} \text{ year}^{-1}$ in 16 years old) than in older stands ($29 \text{ kg N ha}^{-1} \text{ year}^{-1}$ in 31 years old; $24 \text{ kg N ha}^{-1} \text{ year}^{-1}$ in 42

years old; $34 \text{ kg N ha}^{-1} \text{ year}^{-1}$ in 89 years old). In addition, Yang and Chiwa (2021) found that the nitrate concentration in the soil water taken beneath the rooting zone of matured artificial Japanese cedar plantations ($607 \pm 59 \text{ }\mu\text{M}$; 64-69 years old) was significantly higher than that of normal Japanese oak plantations ($8.7 \pm 8.1 \text{ }\mu\text{M}$; 24 years old). Moreover, by adding ammonium nitrate ($50 \text{ kg N ha}^{-1} \text{ year}^{-1}$) to the forest floor directly, Yang and Chiwa (2021) found that the nitrate concentration in the soil water of the matured artificial Japanese cedar plantations increased significantly faster than that of the normal Japanese oak plantations, probably because of the lower N uptake rates in the matured artificial Japanese cedar plantations. Because most of the artificial Japanese cedar/cypress plantations in the FK and MY catchments have reached their maturity (> 50 years; Yang and Chiwa, 2021), the higher proportion of matured artificial Japanese cedar/cypress plantations in the FK1 catchment (Table 1) was highly responsible for the observed elevated leaching of nitrate, caused by the reduction in N uptake rates.

As a result, we concluded that the FK forested catchments were under the high nitrogen saturation stage, FK1 catchment especially, and the nitrogen saturation in the FK1 catchment was responsible for the elevated M_{total} , M_{atm} , $[\text{NO}_3^-]$, $[\text{NO}_3^-]_{\text{atm}}$ found in the stream eluted from the catchment (Figs. 3a, 3b, and 3c).

4.3 The $M_{\text{atm}}/D_{\text{atm}}$ ratio as an index of nitrogen saturation

Past studies have used the concentration of stream nitrate as one of the important

indexes to evaluate the stage of nitrogen saturation in each forest (Aber, 1992; Huang et al., 2020; Rose et al., 2015; Stoddard, 1994). The strong linear relationship ($R^2 = 0.76$; $P < 0.0001$) between the stream nitrate concentration and the $M_{\text{atm}}/D_{\text{atm}}$ ratio, except for the Qingyuan forested catchment (Fig. 3d), further supported that the $M_{\text{atm}}/D_{\text{atm}}$ ratio can be used as an alternative index of nitrogen saturation, as pointed out in Nakagawa et al. (2018).

The differences in the number of storm and/or snowmelt events could affect the $M_{\text{atm}}/D_{\text{atm}}$ ratio as well, because NO_3^- could be injected into the stream water directly, along with the storm / snowmelt water (Tsunogai et al., 2014; Ding et al., 2022; Inamdar and Mitchell, 2006). In recent study, however, we found that the storm events have little impacts on the $M_{\text{atm}}/D_{\text{atm}}$ ratio, based on monitoring temporal variation of $[\text{NO}_3^-]$ in a stream water during storm events (Ding et al., 2022). In addition, the low $M_{\text{atm}}/D_{\text{atm}}$ ratio found in Uryu forested catchment (0.7 %; Table 3) implied that the snowmelt has little impacts on the $M_{\text{atm}}/D_{\text{atm}}$ ratio as well, because 30% of the annual mean precipitation was snow in Uryu forested catchment (Tsunogai et al., 2014).

The differences in the amount of precipitation, temperature, and the flux of stream water could affect the $M_{\text{atm}}/D_{\text{atm}}$ ratio as well. As a result, the annual amount of precipitation, mean temperature, and the annual mean flux of stream water (F_{stream}) in the forested catchments were compiled in Table S2. While the stream nitrate concentration showed the strong linear relationship ($R^2 = 0.76$; $P < 0.0001$) with the $M_{\text{atm}}/D_{\text{atm}}$ ratio (Fig. 3d), the precipitation, temperature, and F_{stream} did not show

significant relationship with the $M_{\text{atm}}/D_{\text{atm}}$ ratio ($P > 0.14$; Fig. 4). As a result, we concluded that the $M_{\text{atm}}/D_{\text{atm}}$ ratio was mainly controlled by the progress of nitrogen saturation, rather than the differences in the number of storm and/or snowmelt events, the amount of precipitation, temperature, and the flux of stream water.

The $M_{\text{atm}}/D_{\text{atm}}$ ratio is a more reliable and robust index than the stream nitrate concentration, as explained below. The Qingyuan forested catchment can be classified into the highest nitrogen saturation stage based only on the highest stream nitrate concentration of $150 \mu\text{M}$ (Table 3). However, based on the leaching flux of nitrogen via stream water monitored by Huang et al. (2020) for 4 years in the Qingyuan forested catchment, along with the deposition flux of nitrogen, we can obtain the $M_{\text{atm}}/D_{\text{atm}}$ ratio in the catchment to be a medium level of $5.8 \pm 1.3 \%$, implying that the nitrogen saturation stage was not so high (Table 3). Huang et al. (2020) also concluded that the input of nitrogen exceeded the output in the catchment, and thus, the catchment was at stage 2 of nitrogen saturation. The $M_{\text{atm}}/D_{\text{atm}}$ ratio in the Qingyuan forested catchment with a medium level among all forested catchments (Fig. 3d) should be a more reliable index of nitrogen saturation.

Compared with those in the other forested catchments in Table 3, the annual amount of precipitation (P) has the lowest value of 709 mm in the Qingyuan forested catchment. The flux of stream water (F_{stream}) has the lowest value of 309 mm as well. Thus, we concluded that nitrate was relatively concentrated in the catchment because of the small precipitation, resulting in relative enrichment in the concentrations of both nitrate (150

μM) and unprocessed atmospheric nitrate (8.9 μM) in the stream.

While the concentration of stream nitrate, as an index of nitrogen saturation traditionally, can be influenced by the amount of precipitation, as demonstrated in the Qingyuan forested catchment, the $M_{\text{atm}}/D_{\text{atm}}$ ratio is independent of the amount of precipitation (Fig. 4). Therefore, the $M_{\text{atm}}/D_{\text{atm}}$ ratio can be used as a more robust index for evaluating nitrogen saturation in each forested catchment.

The only concern on using the $M_{\text{atm}}/D_{\text{atm}}$ ratio as the index of nitrogen saturation is the impact of the differences in the residence time of water in each catchment. The residence time of water varies from 1 month to more than 1 year in forested catchments (Asano et al., 2002; Farrick and Branfireun, 2015; Kabeya et al., 2008; Rodgers et al., 2005; Soulsby et al., 2006; Tetzlaff et al., 2007). The $M_{\text{atm}}/D_{\text{atm}}$ ratio could be lower in catchments with longer residence time of water. We would like to clarify this in future studies by adding much more data of stream nitrate eluted from various forested catchments.

5 Conclusions

Both the concentrations and $\Delta^{17}\text{O}$ of stream nitrate were determined for more than 2 years in the forested catchments of FK (FK1 and FK2) and MY to determine the $M_{\text{atm}}/D_{\text{atm}}$ ratio for each catchment. The FK catchments exhibited higher $M_{\text{atm}}/D_{\text{atm}}$ ratio than the MY catchment and other forested catchments reported in past studies, implying that the progress of nitrogen saturation in the FK catchments was severe. Both age and

proportion of artificial plantation in the FK catchments were responsible for the progress of nitrogen saturation. In addition, although past studies have commonly used the concentration of stream nitrate as an index to evaluate the progress of nitrogen saturation in forested catchments, it can be influenced by the amount of precipitation. As a result, we concluded that the $M_{\text{atm}}/D_{\text{atm}}$ ratio should be used as a more reliable index for evaluating the progress of nitrogen saturation because the $M_{\text{atm}}/D_{\text{atm}}$ ratio is independent from the amount of precipitation.

Data availability. All the primary data are presented in the Supplement. The other data are available upon request to the corresponding author (Weitian Ding).

Author contributions. UT, FN, KS, and MC designed the study. MC and TK performed the field observations. WD, UT, and FN determined the concentrations and isotopic compositions of the samples. WD, TS, FN, and UT performed data analysis, and WD and UT wrote the paper with input from MC, TK, and KS.

Competing interests. The authors declare that they have no conflict of interest.

Acknowledgements.

We thank anonymous referees for valuable remarks on an earlier version of this paper.

We also thank Daisuke Nanki, Takuma Nakamura, and Yuko Muramatsu for their

long-term water sampling. Additionally, we are grateful to the members of the Biogeochemistry Group, Graduate School of Environmental Studies, Nagoya University, for their valuable support throughout this study. This work was supported by a Grant-in-Aid for Scientific Research from the Ministry of Education, Culture, Sports, Science, and Technology of Japan under grant numbers 22H00561, and 17H00780, the Yanmar Environmental Sustainability Support Association, and the River fund of the river foundation, Japan. Weitian Ding would like to take this opportunity to thank the “Nagoya University Interdisciplinary Frontier Fellowship” supported by Nagoya University and JST, the establishment of university fellowships towards the creation of science technology innovation, Grant Number JPMJFS2120.

Reference

- Aber, J. D.: Nitrogen cycling and nitrogen saturation in temperate forest ecosystems, *Trends Ecol. Evol.*, 7(7), 220–224, doi:10.1016/0169-5347(92)90048-G, 1992.
- Aber, J. D., Nadelhoffer, K. J., Steudler, P. and Melillo, J. M.: Nitrogen Saturation in Northern Forest Ecosystems, *Bioscience*, 39(6), 378–386, doi:10.2307/1311067, 1989.
- Aikawa, M., Hiraki, T., Tamaki, M. and Shoga, M.: Difference between filtering-type bulk and wet-only data sets based on site classification, *Atmos. Environ.*, 37(19), 2597–2603, doi:10.1016/S1352-2310(03)00214-0, 2003.
- Alexander, B., Hastings, M. G., Allman, D. J., Dachs, J., Thornton, J. A. and

549 Kunasek, S. A.: Quantifying atmospheric nitrate formation pathways based on a
 550 global model of the oxygen isotopic composition ($\delta^{17}\text{O}$) of atmospheric nitrate,
 551 *Atmos. Chem. Phys.*, 9(14), 5043–5056, doi:10.5194/acp-9-5043-2009, 2009.
 552 Asano, Y., Uchida, T. and Ohte, N.: Residence times and flow paths of water in steep
 553 unchannelled catchments, Tanakami, Japan, *J. Hydrol.*, 261(1–4), 173–192,
 554 doi:10.1016/S0022-1694(02)00005-7, 2002.
 555 Environmental Laboratories Association of Japan: Acid Rain National Survey Report
 556 2017, https://tenbou.nies.go.jp/envgis_explain/acid_rain/content.html.
 557 Bostic, J. T., Nelson, D. M., Sabo, R. D. and Eshleman, K. N.: Terrestrial Nitrogen
 558 Inputs Affect the Export of Unprocessed Atmospheric Nitrate to Surface Waters:
 559 Insights from Triple Oxygen Isotopes of Nitrate, *Ecosystems*, doi:10.1007/s10021-
 560 021-00722-9, 2021.
 561 Bourgeois, I., Savarino, J., Némery, J., Caillon, N., Albertin, S., Delbart, F., Voisin,
 562 D. and Clément, J. C.: Atmospheric nitrate export in streams along a montane to
 563 urban gradient, *Sci. Total Environ.*, 633, 329–340,
 564 doi:10.1016/j.scitotenv.2018.03.141, 2018a.
 565 Bourgeois, I., Savarino, J., Caillon, N., Angot, H., Barbero, A., Delbart, F., Voisin, D.
 566 and Clément, J. C.: Tracing the Fate of Atmospheric Nitrate in a Subalpine Watershed
 567 Using $\Delta^{17}\text{O}$, *Environ. Sci. Technol.*, 52(10), 5561–5570, doi:10.1021/acs.est.7b02395,
 568 2018b. Chiwa, M.: Ten-year determination of atmospheric phosphorus deposition at
 569 three forested sites in Japan, *Atmos. Environ.*, 223(May 2019), 1–7,

doi:10.1016/j.atmosenv.2019.117247, 2020.

Chiwa, M.: Long-term changes in atmospheric nitrogen deposition and stream water nitrate leaching from forested watersheds in western Japan, *Environ. Pollut.*, 287(November 2020), 117634, doi:10.1016/j.envpol.2021.117634, 2021.

Chiwa, M., Enoki, T., Higashi, N., Kumagai, T. and Otsuki, K.: The Increased Contribution of Atmospheric Nitrogen Deposition to Nitrogen Cycling in a Rural Forested Area of Kyushu, Japan, *Water, Air, Soil Pollut.*, 224(11), 1763, doi:10.1007/s11270-013-1763-2, 2013.

Chiwa, M., Onikura, N., Ide, J. and Kume, A.: Impact of N-Saturated Upland Forests on Downstream N Pollution in the Tatara River Basin, Japan, *Ecosystems*, 15(2), 230–241, doi:10.1007/s10021-011-9505-z, 2012.

Chiwa, M.: Characteristics of atmospheric nitrogen and sulfur containing compounds in an inland suburban-forested site in northern Kyushu, western Japan, *Atmos. Res.*, 96(4), 531–543, doi:10.1016/j.atmosres.2010.01.001, 2010.

Ding, W., Tsunogai, U., Nakagawa, F., Sambuichi, T., Sase, H., Morohashi, M., and Yotsuyanagi, H.: Tracing the source of nitrate in a forested stream showing elevated concentrations during storm events, *Biogeosciences*, 19, 3247–3261, <https://doi.org/10.5194/bg-19-3247-2022>, 2022.

Endo, T., Yagoh, H., Sato, K., Matsuda, K., Hayashi, K., Noguchi, I. and Sawada, K.: Regional characteristics of dry deposition of sulfur and nitrogen compounds at

590 EANET sites in Japan from 2003 to 2008, *Atmos. Environ.*, 45(6), 1259–1267,
 591 doi:10.1016/j.atmosenv.2010.12.003, 2011.

592 Farrick, K. K. and Branfireun, B. A.: Flowpaths, source water contributions and water
 593 residence times in a Mexican tropical dry forest catchment, *J. Hydrol.*, 529, 854–865,
 594 doi:10.1016/j.jhydrol.2015.08.059, 2015. Kabeya, N., Shimizu, A., Nobuhiro, T. and
 595 Tamai, K.: Preliminary study of flow regimes and stream water residence times in
 596 multi-scale forested watersheds of central Cambodia, *Paddy Water Environ.*, 6(1), 25–
 597 35, doi:10.1007/s10333-008-0104-3, 2008.

598 Fukushima, K., Tateno, R. and Tokuchi, N.: Soil nitrogen dynamics during stand
 599 development after clear-cutting of Japanese cedar (*Cryptomeria japonica*) plantations,
 600 *J. For. Res.*, 16(5), 394–404, doi:10.1007/s10310-011-0286-1, 2011.

601 Galloway, J. N., Aber, J. D., Erisman, J. W., Seitzinger, S. P., Howarth, R. W.,
 602 Cowling, E. B. and Cosby, B. J.: The nitrogen cascade, *Bioscience*, 53(4), 341–356,
 603 doi:10.1641/0006-3568(2003)053[0341:TNC]2.0.CO;2, 2003.

604 Hattori, S., Nuñez Palma, Y., Itoh, Y., Kawasaki, M., Fujihara, Y., Takase, K. and
 605 Yoshida, N.: Isotopic evidence for seasonality of microbial internal nitrogen cycles in
 606 a temperate forested catchment with heavy snowfall, *Sci. Total Environ.*, 690, 290–
 607 299, doi:10.1016/j.scitotenv.2019.06.507, 2019.

608 Hirota, A., Tsunogai, U., Komatsu, D. D. and Nakagawa, F.: Simultaneous
 609 determination of $\delta^{15}\text{N}$ and $\delta^{18}\text{O}$ of N_2O and $\delta^{13}\text{C}$ of CH_4 in nanomolar quantities from
 610 a single water sample, *Rapid Commun. Mass Spectrom.*, 24, 1085–1092,

doi:10.1002/rcm.4483, 2010.

Huang, S., Wang, F., Elliott, E. M., Zhu, F., Zhu, W., Koba, K., Yu, Z., Hobbie, E. A., Michalski, G., Kang, R., Wang, A., Zhu, J., Fu, S. and Fang, Y.: Multiyear Measurements on $\Delta^{17}\text{O}$ of Stream Nitrate Indicate High Nitrate Production in a Temperate Forest, *Environ. Sci. Technol.*, 54(7), 4231–4239, doi:10.1021/acs.est.9b07839, 2020.

Inoue, T., Nakagawa, F., Shibata, H. and Tsunogai, U.: Vertical Changes in the Flux of Atmospheric Nitrate From a Forest Canopy to the Surface Soil Based on $\Delta^{17}\text{O}$ Values, *J. Geophys. Res. Biogeosciences*, 126(4), 1–18, doi:10.1029/2020JG005876, 2021.

Inamdar, S. P. and Mitchell, M. J.: Hydrologic and topographic controls on storm-event exports of dissolved organic carbon (BOC) and nitrate across catchment scales, *Water Resour. Res.*, 42(3), 1–16, doi:10.1029/2005WR004212, 2006.

Kaiser, J., Hastings, M. G., Houlton, B. Z., Röckmann, T. and Sigman, D. M.: Triple oxygen isotope analysis of nitrate using the denitrifier method and thermal decomposition of N_2O , *Anal. Chem.*, 79(2), 599–607, doi:10.1021/ac061022s, 2007.

Komatsu, D. D., Ishimura, T., Nakagawa, F. and Tsunogai, U.: Determination of the $^{15}\text{N}/^{14}\text{N}$, $^{17}\text{O}/^{16}\text{O}$, and $^{18}\text{O}/^{16}\text{O}$ ratios of nitrous oxide by using continuous-flow isotope-ratio mass spectrometry Daisuke, *Rapid Commun. Mass Spectrom.*, 22, 1587–1596, doi:10.1002/rcm.3493, 2008a.

Komatsu, H., Maita, E. and Otsuki, K.: A model to estimate annual forest

632 evapotranspiration in Japan from mean annual temperature, , 330–340,
 633 doi:10.1016/j.jhydrol.2007.10.006, 2008b.
 634 Konno, U., Tsunogai, U., Komatsu, D. D., Daita, S., Nakagawa, F., Tsuda, A.,
 635 Matsui, T., Eum, Y. J. and Suzuki, K.: Determination of total N₂ fixation rates in the
 636 ocean taking into account both the particulate and filtrate fractions, *Biogeosciences*,
 637 7(8), 2369–2377, doi:10.5194/bg-7-2369-2010, 2010.
 638 Matsuda, K.: Estimation of dry deposition for sulfur and nitrogen compounds in the
 639 atmosphere : Updated parameterization of deposition velocity, *J. Japan Soc. Atmos.*
 640 *Environ.*, 43(6), 332–339, doi:10.11298/taiki1995.43.332, 2008.
 641 McIlvin, M. R. and Altabet, M. A.: Chemical conversion of nitrate and nitrite to
 642 nitrous oxide for nitrogen and oxygen isotopic analysis in freshwater and seawater,
 643 *Anal. Chem.*, 77(17), 5589–5595, doi:10.1021/ac050528s, 2005.
 644 Michalski, G., Scott, Z., Kabling, M. and Thiemens, M. H.: First measurements and
 645 modeling of $\Delta^{17}\text{O}$ in atmospheric nitrate, *Geophys. Res. Lett.*, 30(16), 3–6,
 646 doi:10.1029/2003GL017015, 2003.
 647 Michalski, G., Meixner, T., Fenn, M., Hernandez, L., Sirulnik, A., Allen, E. and
 648 Thiemens, M.: Tracing Atmospheric Nitrate Deposition in a Complex Semiarid
 649 Ecosystem Using $\Delta^{17}\text{O}$, *Environ. Sci. Technol.*, 38(7), 2175–2181,
 650 doi:10.1021/es034980+, 2004.
 651 Mitchell, M. J., Iwatsubo, G., Ohnishi, K. and Nakagawa, Y.: Nitrogen saturation in
 652 Japanese forests: An evaluation, *For. Ecol. Manage.*, 97(1), 39–51,

doi:10.1016/S0378-1127(97)00047-9, 1997.

Morin, S., Sander, R. and Savarino, J.: Simulation of the diurnal variations of the oxygen isotope anomaly ($\Delta^{17}\text{O}$) of reactive atmospheric species, *Atmos. Chem. Phys.*, 11(8), 3653–3671, doi:10.5194/acp-11-3653-2011, 2011.

Nakagawa, F., Suzuki, A., Daita, S., Ohyama, T., Komatsu, D. D. and Tsunogai, U.: Tracing atmospheric nitrate in groundwater using triple oxygen isotopes: Evaluation based on bottled drinking water, *Biogeosciences*, 10(6), 3547–3558, doi:10.5194/bg-10-3547-2013, 2013.

Nakagawa, F., Tsunogai, U., Obata, Y., Ando, K., Yamashita, N., Saito, T., Uchiyama, S., Morohashi, M. and Sase, H.: Export flux of unprocessed atmospheric nitrate from temperate forested catchments: A possible new index for nitrogen saturation, *Biogeosciences*, 15(22), 7025–7042, doi:10.5194/bg-15-7025-2018, 2018.

Nelson, D. M., Tsunogai, U., Ding, D., Ohyama, T., Komatsu, D. D., Nakagawa, F., Noguchi, I. and Yamaguchi, T.: Triple oxygen isotopes indicate urbanization affects sources of nitrate in wet and dry atmospheric deposition, *Atmos. Chem. Phys.*, 18(9), 6381–6392, doi:10.5194/acp-18-6381-2018, 2018.

Ohrui, K. and Mitchell, M. J.: Nitrogen Saturation in Japanese Forested Watersheds
 Author (s): Kiyokazu Ohrui and Myron J . Mitchell Published by : Wiley Stable
 URL : <http://www.jstor.org/stable/2269507> Accessed : 05-07-2016 04 : 51 UTC Your use of the JSTOR archive indicates your ac , 7(2), 391–401, 1997.

Paerl, H. W. and Huisman, J.: Climate change: A catalyst for global expansion of

674 harmful cyanobacterial blooms, *Environ. Microbiol. Rep.*, 1(1), 27–37,
675 doi:10.1111/j.1758-2229.2008.00004.x, 2009.

676 Peterjohn, W. T., Adams, M. B. and Gilliam, F. S.: Symptoms of nitrogen saturation
677 in two central Appalachian hardwood forest ecosystems, *Biogeochemistry*, 35(3),
678 507–522, doi:10.1007/BF02183038, 1996.

679 Riha, K. M., Michalski, G., Gallo, E. L., Lohse, K. A., Brooks, P. D. and Meixner, T.:
680 High Atmospheric Nitrate Inputs and Nitrogen Turnover in Semi-arid Urban
681 Catchments, *Ecosystems*, 17(8), 1309–1325, doi:10.1007/s10021-014-9797-x, 2014.

682 Rodgers, P., Soulsby, C., Waldron, S. and Tetzlaff, D.: Using stable isotope tracers to
683 identify hydrological flow paths, residence times and landscape controls in a
684 mesoscale catchment, *Hydrol. Earth Syst. Sci. Discuss.*, 9, 139–155, 2005.

685 Rose, L. A., Elliott, E. M. and Adams, M. B.: Triple Nitrate Isotopes Indicate Differing Nitrate
686 Source Contributions to Streams Across a Nitrogen Saturation Gradient, *Ecosystems*,
687 18(7), 1209–1223, doi:10.1007/s10021-015-9891-8, 2015.

688 Sabo, R. D., Nelson, D. M. and Eshleman, K. N.: Episodic, seasonal, and annual
689 export of atmospheric and microbial nitrate from a temperate forest, *Geophys. Res.*
690 *Lett.*, 43(2), 683–691, doi:10.1002/2015GL066758, 2016.

691 Sappa, G., Ferranti, F. and Pecchia, G. M.: Validation Of Salt Dilution Method For
692 Discharge Measurements In The Upper Valley Of Aniene River (Central Italy), *Recent*
693 *Adv. Environ. Ecosyst. Dev.*, (October 2015), 42–48, 2015.

694 Soulsby, C., Tetzlaff, D., Rodgers, P., Dunn, S. and Waldron, S.: Runoff processes,

695 stream water residence times and controlling landscape characteristics in a mesoscale
 696 catchment: An initial evaluation, *J. Hydrol.*, 325(1–4), 197–221,
 697 doi:10.1016/j.jhydrol.2005.10.024, 2006.
 698 Stoddard, J. L.: Long-Term Changes in Watershed Retention of Nitrogen, , 223–284,
 699 doi:10.1021/ba-1994-0237.ch008, 1994.
 700 Tetzlaff, D., Malcolm, I. A. and Soulsby, C.: Influence of forestry, environmental
 701 change and climatic variability on the hydrology, hydrochemistry and residence times
 702 of upland catchments, *J. Hydrol.*, 346(3–4), 93–111,
 703 doi:10.1016/j.jhydrol.2007.08.016, 2007.
 704 Tsunogai, U., Komatsu, D. D., Daita, S., Kazemi, G. A., Nakagawa, F., Noguchi, I.
 705 and Zhang, J.: Tracing the fate of atmospheric nitrate deposited onto a forest
 706 ecosystem in Eastern Asia using $\Delta^{17}\text{O}$, *Atmos. Chem. Phys.*, 10(4), 1809–1820,
 707 doi:10.5194/acp-10-1809-2010, 2010.
 708 Tsunogai, U., Daita, S., Komatsu, D. D., Nakagawa, F. and Tanaka, A.: Quantifying
 709 nitrate dynamics in an oligotrophic lake using $\Delta^{17}\text{O}$, *Biogeosciences*, 8(3), 687–702,
 710 doi:10.5194/bg-8-687-2011, 2011.
 711 Tsunogai, U., Komatsu, D. D., Ohyama, T., Suzuki, A., Nakagawa, F., Noguchi, I.,
 712 Takagi, K. and Nomura, M.: Quantifying the effects of clear-cutting and strip-cutting
 713 on nitrate dynamics in a forested watershed using triple oxygen isotopes as tracers, ,
 714 (1), 5411–5424, doi:10.5194/bg-11-5411-2014, 2014.
 715 Tsunogai, U., Miyauchi, T., Ohyama, T., Komatsu, D. D., Nakagawa, F., Obata, Y.,

Sato, K. and Ohizumi, T.: Accurate and precise quantification of atmospheric nitrate in streams draining land of various uses by using triple oxygen isotopes as tracers, *Biogeosciences*, 13(11), 3441–3459, doi:10.5194/bg-13-3441-2016, 2016.

Tsunogai, U., Miyauchi, T., Ohyama, T., Komatsu, D. D., Ito, M. and Nakagawa, F.: Quantifying nitrate dynamics in a mesotrophic lake using triple oxygen isotopes as tracers, *Limnol. Oceanogr.*, 63, S458–S476, doi:10.1002/lno.10775, 2018.

Vitousek, P. M. and Howarth, R. W.: Nitrogen limitation on land and in the sea: How can it occur?, *Biogeochemistry*, 13(2), 87–115, doi:10.1007/BF00002772, 1991.

Watanabe, M., Miura, S., Hasegawa, S., Koshikawa, M. K., Takamatsu, T., Kohzu, A., Imai, A. and Hayashi, S.: Coniferous coverage as well as catchment steepness influences local stream nitrate concentrations within a nitrogen-saturated forest in central Japan, *Sci. Total Environ.*, 636, 539–546, doi:10.1016/j.scitotenv.2018.04.307, 2018.

Yamazaki, A., Watanabe, T. and Tsunogai, U.: Nitrogen isotopes of organic nitrogen in reef coral skeletons as a proxy of tropical nutrient dynamics, *Geophys. Res. Lett.*, 38(19), 1–5, doi:10.1029/2011GL049053, 2011.

Yang, R. and Chiwa, M.: Low nitrogen retention in a Japanese cedar plantation in a suburban area, western Japan, *Sci. Rep.*, 11(1), 1–7, doi:10.1038/s41598-021-84753-1, 2021.

737

738

739

740 **Table 1.** Plant information for each forested catchment (Chiwa, 2021).

Overstory vegetation (%)	FK1	FK2	MY
Artificial Japanese cedar/cypress plantation	74	40	16
Other artificial coniferous plantations	<1	<1	7
Natural trees	10	54	75
Others	16	5	2

741

742

743

744 **Table 2.** Average concentrations of stream nitrate ($[\text{NO}_3^-]_{\text{avg}}$), the average
745 concentrations of unprocessed NO_3^- in streams ($[\text{NO}_3^-]_{\text{atm}}$), the annual export flux
746 of NO_3^- per unit area of catchments (M_{total}), the annual export flux of NO_3^- per unit
747 area of catchments (M_{atm}), the deposition flux of NO_3^- per unit area of catchment
748 (D_{atm}), and the $M_{\text{atm}}/D_{\text{atm}}$ ratios in the study catchments.

	FK1	FK2	MY
$[\text{NO}_3^-]_{\text{avg}}$ (μM)	109.5	90.9	7.3
$[\text{NO}_3^-]_{\text{atm}}$ (μM)	10.80 ± 1.65	5.06 ± 0.92	0.16 ± 0.05
M_{total} ($\text{mmol m}^{-2} \text{yr}^{-1}$)	98.8 ± 17.8	82.0 ± 14.8	23.7 ± 1.2
M_{atm} ($\text{mmol m}^{-2} \text{yr}^{-1}$)	9.7 ± 2.3	4.6 ± 1.2	0.5 ± 0.2
D_{atm} ($\text{mmol m}^{-2} \text{yr}^{-1}$)	69.3 ± 13.9	69.3 ± 13.9	40.1 ± 8.0
$M_{\text{atm}}/D_{\text{atm}}$ (%)	14.1 ± 4.4	6.6 ± 2.1	1.3 ± 0.5

749

Table 3. The annual amount of precipitation (P), the average concentration of stream nitrate ($[\text{NO}_3^-]_{\text{avg}}$), the nitrogen saturation stage, the average concentration of unprocessed NO_3^- in streams ($[\text{NO}_3^-]_{\text{atm}}$), the annual export flux of NO_3^- per unit area of catchment (M_{total}), the annual export flux of NO_3^- per unit area of catchment (M_{atm}), the deposition flux of NO_3^- per unit area of catchment (D_{atm}), and the $M_{\text{atm}}/D_{\text{atm}}$ ratio in the FK1, FK2, and MY, along with those in the catchments studied in past studies using $\Delta^{17}\text{O}$ of nitrate as a tracer.

	P	$[\text{NO}_3^-]_{\text{avg}}$	N stage*	$[\text{NO}_3^-]_{\text{atm}}$	M_{atm}	M_{total}	D_{atm}	$M_{\text{atm}}/D_{\text{atm}}$
	mm	μM		μM	$\text{mmol m}^{-2} \text{yr}^{-1}$			%
FK1 ^a	1777	109.5	-	10.8	9.7	98.8	69.3	14.1
FK2 ^a	1777	90.9	-	5.06	4.6	82.0	69.3	6.6
MY ^a	3981	7.3	-	0.2	0.5	23.7	40.1	1.3
KJ ^b	2500	58.4	-	3.3	4.3	76.4	45.6	9.4
IJ1 ^b	3300	24.4	2	1.4	2.9	50.1	44.5	6.5
IJ2 ^b	3300	17.1	-	0.6	1.2	35.1	44.5	2.6
Fernow1 ^c	1450	17.9	1	1.6	0.8	9.3	23.4	3.6
Fernow2 ^c	1450	34.3	2	3.4	1.5	14.8	23.4	6.3
Fernow3 ^c	1450	60.0	3	4.2	2.4	34.5	23.4	10.3
Uryu ^d	1170	0.7	-	0.1	0.1	1.0	18.6	0.7
Qingyuan ^e	709	150.0	2	8.9	2.9	49.3	50.0	5.8

a: This study

b: Nakagawa et al., 2018; Nakahara et al., 2010

c: Rose et al., 2015

d: Tsunogai et al., 2014

e: Huang et al., 2020

*: N saturation stage estimated in past studies

-: No data

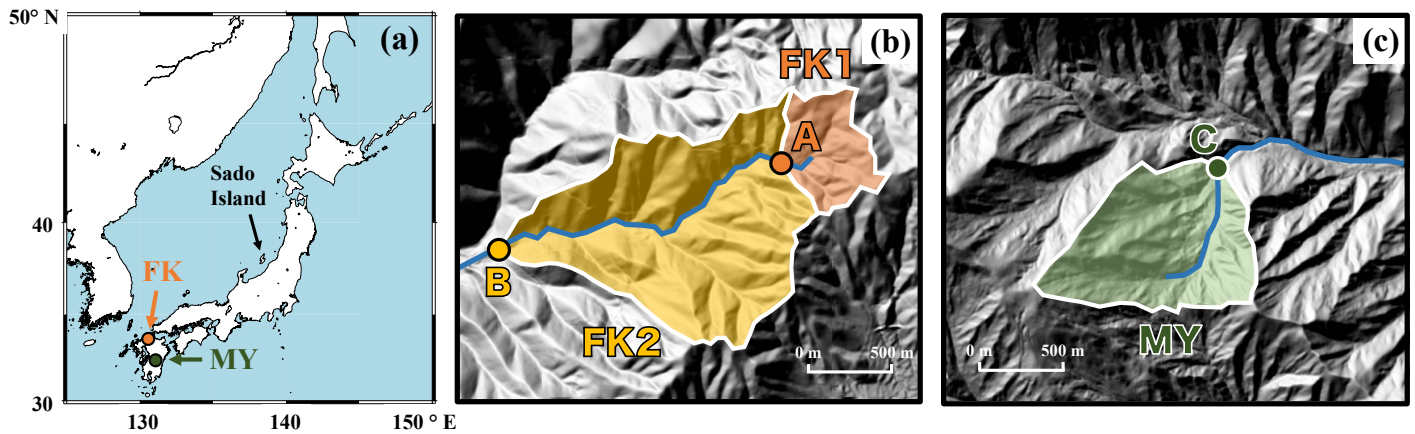


Figure 1. A map showing the locations of the study catchments (FK and MY) in Japan (a), and the maps of FK1, FK2 (b) and MY catchments (c), shown by orange, yellow, and green areas, respectively, together with the sampling station A, B, and C, respectively, shown by orange, yellow, and green circles, respectively.

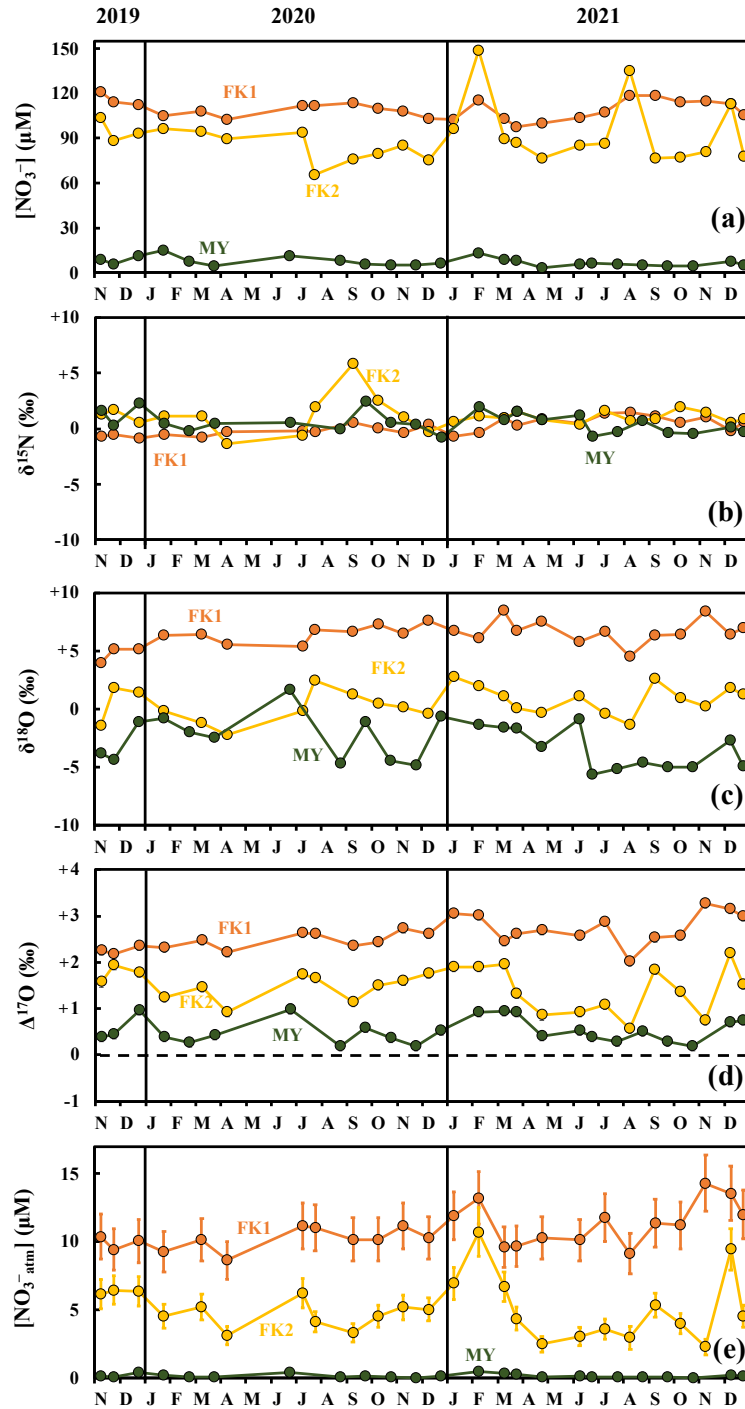
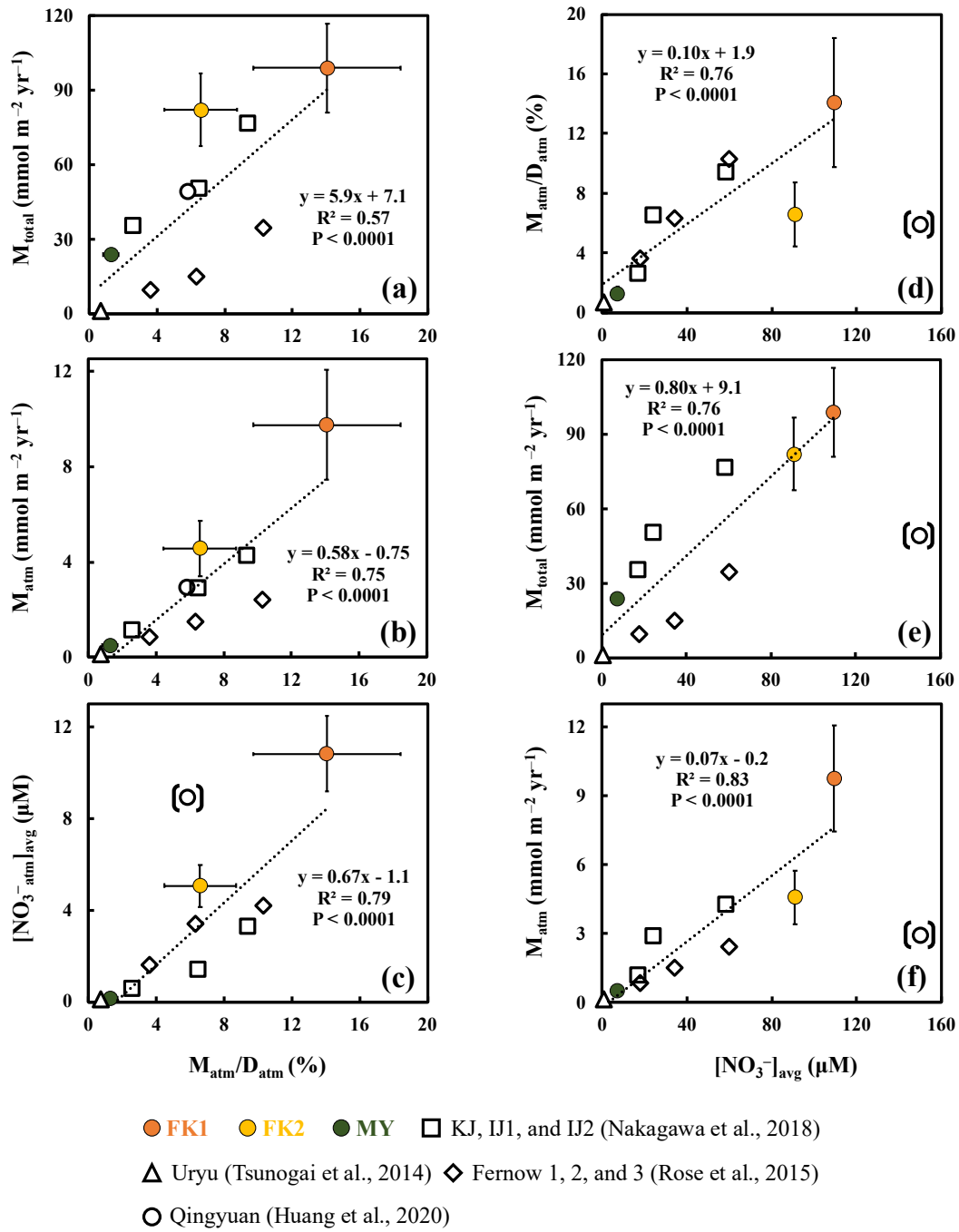


Figure 2. Temporal variations in concentrations of stream nitrate (FK1: orange circles; FK2: yellow circles; MY: green circles) (a), together with those in $\delta^{15}\text{N}$ (b), $\delta^{18}\text{O}$ (c), and $\Delta^{17}\text{O}$ (d) of nitrate, and the concentration of unprocessed $\text{NO}_3^-_{\text{atm}}$ ($[\text{NO}_3^-_{\text{atm}}]$) (e) in the stream water of the FK1, FK2, and MY forested catchments. Error bars smaller than the sizes of the symbols are not presented.



785 **Figure 3.** Annual export flux of nitrate per unit area (M_{total}) plotted as a function of the
 786 $M_{\text{atm}}/D_{\text{atm}}$ ratio in each forested catchment (a); the annual export flux of unprocessed
 787 atmospheric nitrate per unit area (M_{atm}) plotted as a function of the $M_{\text{atm}}/D_{\text{atm}}$ ratio (b);
 788 the average concentration of NO_3^- ($[\text{NO}_3^-]_{\text{atm}}$) plotted as a function of the
 789 $M_{\text{atm}}/D_{\text{atm}}$ ratio (c); the $M_{\text{atm}}/D_{\text{atm}}$ ratio plotted as a function of the average concentration

of nitrate ($[\text{NO}_3^-]_{\text{avg}}$) (d); the M_{total} plotted as a function of $[\text{NO}_3^-]_{\text{avg}}$ (e); the M_{atm} plotted as a function of $[\text{NO}_3^-]_{\text{avg}}$ (f) (FK1: orange circles; FK2: yellow circles; MY: green circles). Those determined for the forested catchments in past studies are plotted as well (Qingyuan: white circle (Huang et al., 2020); KJ, IJ1, and IJ2: white squares (Nakagawa et al., 2018); Fernow 1, 2, and 3: white diamonds (Lucy et al., 2015); Uryu: white triangle (Tsunogai., 2014)). The data obtained in the Qingyuan forested catchment are shown in parentheses and excluded from the calculation to estimate correlation coefficients (see text for the reason).

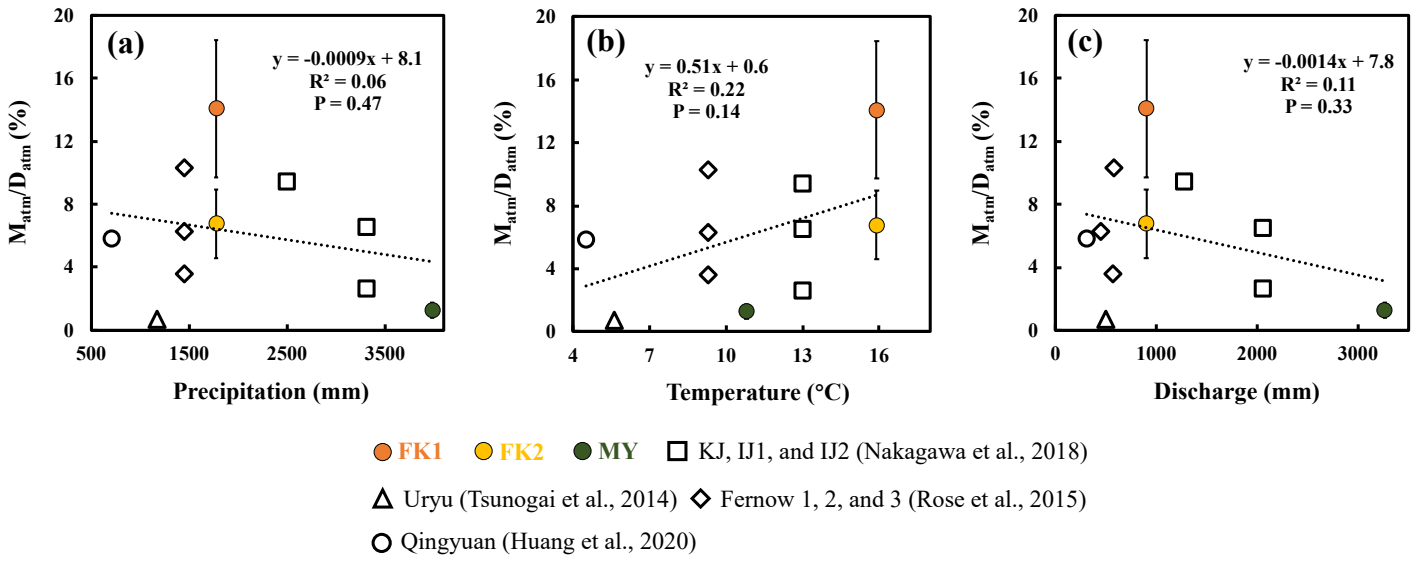


Figure 4. the M_{atm}/D_{atm} ratio plotted as a function of the amount of precipitation (a), the M_{atm}/D_{atm} ratio plotted as a function of the temperature (b), and the M_{atm}/D_{atm} ratio plotted as a function of flux of stream water (c) (FK1: orange circles; FK2: yellow circles; MY: green circles). Those determined for the forested catchments in past studies are plotted as well.

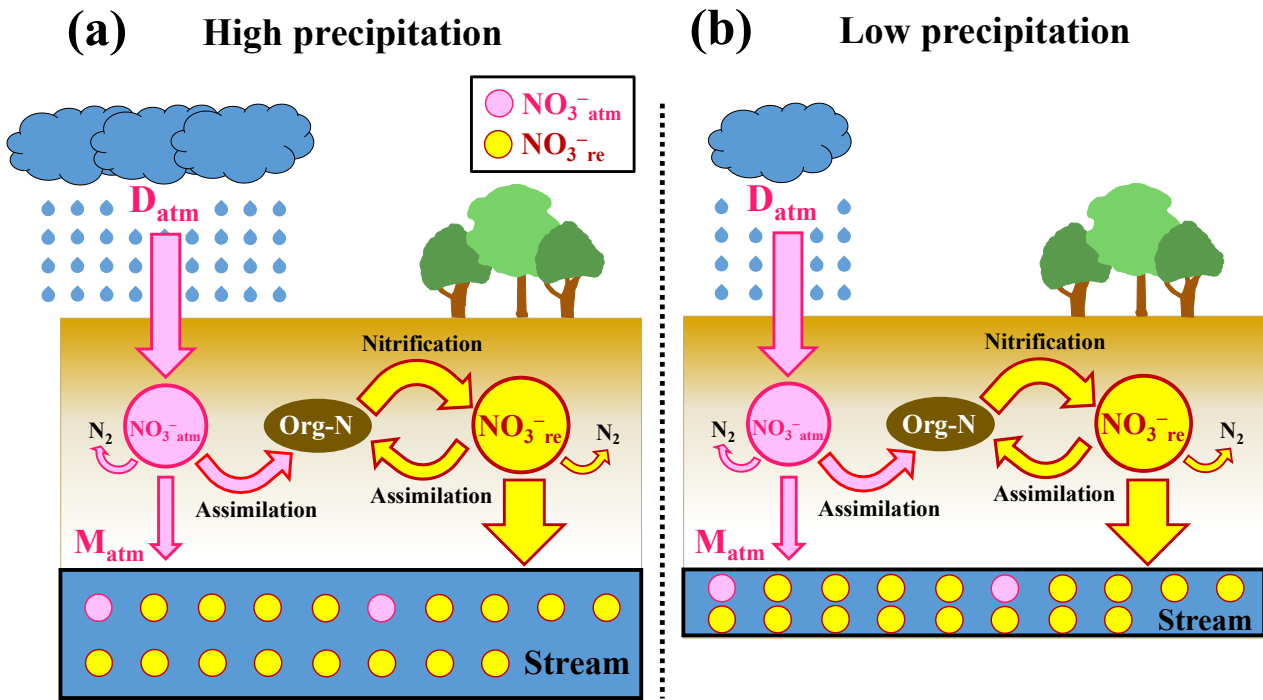


Figure 5. Schematic diagram showing the biogeochemical processing of nitrate in forested catchments under high precipitation (a) and low precipitation (b), where $\text{NO}_3^-_{\text{atm}}$ (unprocessed atmospheric nitrate) is represented by pink circles, $\text{NO}_3^-_{\text{re}}$ by yellow circles, the flows of $\text{NO}_3^-_{\text{atm}}$ by pink arrows, and those of $\text{NO}_3^-_{\text{re}}$ (remineralized nitrate) by yellow arrows (modified after Nakagawa., 2018). Although the deposition rates of $\text{NO}_3^-_{\text{atm}}$ (D_{atm}) and the biogeochemical reaction rates between (a) and (b) are the same, we can expect high $[\text{NO}_3^-]$ in (b). On the other hand, the $M_{\text{atm}}/D_{\text{atm}}$ ratio between (a) and (b) are the same.